

Control of delay-induced oscillation death by coupling phase in coupled oscillatorsWei Zou,^{1,2,3,*} Jianquan Lu,^{3,4} Yang Tang,^{2,3,5} Chengjian Zhang,¹ and Jürgen Kurths^{2,3,6}¹*School of Mathematics and Statistics, Huazhong University of Science and Technology, Wuhan 430074, China*²*Institute of Physics, Humboldt University Berlin, Berlin D-12489, Germany*³*Potsdam Institute for Climate Impact Research, Telegraphenberg, Potsdam D-14415, Germany*⁴*Department of Mathematics, Southeast University, Nanjing 210096, China*⁵*Space Control and Inertial Technology Research Center, Harbin Institute of Technology, Harbin 150001, China*⁶*Institute for Complex systems and Mathematical Biology, University of Aberdeen, Aberdeen AB24 3FX, UK*

(Received 4 August 2011; revised manuscript received 10 October 2011; published 20 December 2011)

A coupling phase is deemed to be crucial in stabilizing behavior in nonlinear systems. In this paper, we study how the coupling phase influences the delay-induced oscillation death (OD) in coupled oscillators. The OD boundaries are identified analytically even in the presence of the coupling phase. We find that OD only occurs for a coupling phase belonging to a certain interval. The optimal coupling phase, under which the largest OD island forms, is characterized well by a power law scaling with respect to the frequency. The coupling phase turns out to be a key parameter that determines a delay-induced OD. Furthermore, the controlling role of the coupling phase generally is proved to hold fairly for networked delay-coupled oscillators.

DOI: [10.1103/PhysRevE.84.066208](https://doi.org/10.1103/PhysRevE.84.066208)

PACS number(s): 05.45.Xt, 87.10.-e

I. INTRODUCTION

Collective emergent behaviors are omnipresent in biology, chemistry, and physics. To characterize such phenomena, systems of coupled nonlinear oscillators provide one of the basic models for performing the studies [1–5]. A typical collective behavior is *oscillation death* (OD), which refers to a phenomenon that coupled oscillatory systems stop oscillating and asymptotically go to a fixed point. OD is of interest and importance because it is expected to play a constructive role in realizing important functions of many real systems, such as synthetic genetic networks [6,7] and yeast [8]. Generally, a parameter mismatch [9–13] or a time-delay coupling [14–16] is the typical requisite condition for OD to occur in coupled nonlinear oscillators. Besides the above two general conditions, dynamic coupling [17] or conjugate coupling [18,19] also can induce OD behavior.

OD induced by delay was realized by Reddy *et al.* [14–16] and immediately was observed in an experiment of electronic circuits [20]. Since then, considerable interest arose in delay-induced OD. Furthermore, for instance, it was recognized experimentally in coupled living oscillators [21], thermo-optical oscillators [22], and lasers [23]. Recent papers proposed many forms of delayed coupling, which can lead to OD, such as distributed delays [24], partial time-delay coupling [25], gradient time-delay coupling [26], and integrative time-delay coupling [27]. OD in delay-coupled networks also has received increasing attention [28,29]. All the papers about delay-induced OD demonstrate that delayed coupling can nicely ensure the stability of the fixed point, which is unstable in the uncoupled system. Recently, delayed coupling also was shown to be effective in stabilizing the inherently unstable periodic orbit in two coupled oscillators [30].

Now, the importance of delay-induced OD is uncovered gradually, and, so far, all the previous papers have been restricted to real coupling strength. By introducing the phase

of coupling, the coupling could even become complex, which is termed phase-dependent coupling [3,4]. The importance of the coupling phase has been indicated well in optical systems with delayed feedback control where the feedback phase is supposed to be related to the phase of the complex electric field [3,4]. An experimental realization of such a complex coupling scheme is feasible by tuning the distance between the integrated tandem laser and an external Fabry-Pérot etalon [31]. The dynamics of phase-dependently coupled lasers has been studied numerically in Ref. [32]. By considering different models of coupled bursting neurons [33], the coupling phase is verified to be important in suppressing pathological brain rhythms. Furthermore, the coupling phase parameter recently has been shown to be essential in organizing the system's dynamics, such as in refuting the odd-number limitation of delayed feedback control [34], designing a long-term chaotic anticipating synchronization [35], and controlling the stability of splay states [36].

Until now, effects of the coupling phase on delay-induced OD were not well examined, although delayed coupling is believed to switch the stability features of a system [37]. In this paper, we explore delay-induced OD in the presence of the coupling phase and find that the existence and the maximization of OD islands in the parameter space can be controlled well by the coupling phase. The coupling phase is found to be a key parameter for the phenomenon of OD induced by time delay.

The remainder of the paper starts from two delay-coupled oscillators in Sec. II, and then Sec. III extends the studies to networked delay-coupled oscillators. Finally, a conclusion and discussions are given in Sec. IV.

II. TWO DELAY-COUPLED OSCILLATORS

Consider the following two delay-coupled Landau-Stuart oscillators:

$$\dot{z}_j(t) = [1 + iw - |z_j(t)|^2]z_j(t) + Ke^{i\theta}[z_s(t - \tau) - z_j(t)] \quad (1)$$

*zouwei2010@mail.hust.edu.cn

for $j, s = 1$ or 2 , where z_1, z_2 are complex variables that represent the state of the corresponding oscillators, w is the frequency, K ($K > 0$) and θ ($-\pi < \theta \leq \pi$) are the coupling strength and the coupling phase, respectively, and τ is the propagation delay. In the absence of coupling (i.e., $K = 0$), each uncoupled oscillator performs the same limit-cycle motion $z = e^{iwt}$. When coupling is switched on (i.e., $K > 0$), the occurrence of OD implies the conversion of stability of the fixed point by delayed coupling.

The Landau-Stuart model, as a standard form of the supercritical Hopf bifurcation, has been considered as a paradigm for oscillators [2]. Already, rich dynamics in the model of coupled Landau-Stuart oscillators have been investigated extensively. Especially, the Landau-Stuart limit-cycle oscillator successfully has served as a typical model for studying the OD phenomenon in the field of nonlinear dynamics for more than two decades [9–27]. In order to make it easier to compare our papers with the previous papers [14–16], the Landau-Stuart model also is employed in this paper.

Already, the OD state $z_1 = z_2 = 0$ is an equilibrium point of the coupled system (1), thus, the delayed coupling simply converts its stability from unstable to stable or vice versa. To obtain stability domains of an OD state, a linear stability analysis of Eq. (1) around the origin ($z_1 = z_2 = 0$) can be carried out. Assuming that the linear perturbations vary as $e^{\lambda t}$, we get the following stability matrix:

$$M = \begin{pmatrix} 1 - Ke^{i\theta} + iw & Ke^{i\theta}e^{-\lambda\tau} \\ Ke^{i\theta}e^{-\lambda\tau} & 1 - Ke^{i\theta} + iw \end{pmatrix}, \quad (2)$$

where λ is the eigenvalue of M . If all real parts of the eigenvalues of the stability matrix M are negative, OD can occur. Mainly following the procedures of Reddy *et al.* [14,15] and Dodla *et al.* [16], the two boundary curves of OD regions are derived as

$$\begin{aligned} \tau_1(K, \theta) &= \frac{\theta + \cos^{-1}\left(\frac{K \cos \theta - 1}{K}\right)}{w - K \sin \theta - \sqrt{K^2 - (K \cos \theta - 1)^2}}, \\ \tau_2(K, \theta) &= \frac{\pi + \theta - \cos^{-1}\left(\frac{K \cos \theta - 1}{K}\right)}{w - K \sin \theta + \sqrt{K^2 - (K \cos \theta - 1)^2}}, \end{aligned} \quad (3)$$

which is reduced to the results in Ref. [14] when $\theta = 0$.

Obviously, the coupling phase θ is involved to form death critical curves. As a first insight into the two critical curves given by Eq. (3), we have shown results for $\theta = -0.1\pi$ and $\theta = 0.1\pi$ in Fig. 1. $w = 10$ is fixed. The OD regions are enclosed by the two critical curves of $\tau_1(K, \theta)$ (the solid line) and $\tau_2(K, \theta)$ (the dotted line). These theoretical OD regions have been checked well by our numerical results represented by the open circles, which are obtained from numerically integrating the coupled system (1). For other parameters, we get similar results.

Next, we investigate the effect of the coupling phase on OD islands by calculating the two critical curves for different θ 's in Eq. (3). Furthermore, Fig. 2 shows several OD islands for different coupling phases in the parameter space $[\tau, \log_{10}(K)]$. $w = 10$. We find that the OD islands monotonically shrink with increasing the coupling phase θ from zero and first grow and then shrink with decreasing the coupling phase from zero. Since OD is a special in-phase state, the changing behavior

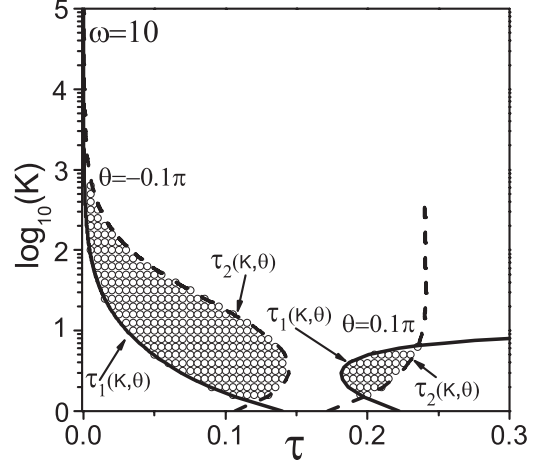


FIG. 1. The OD islands of the coupled system (1) in the parameter space $[\tau, \log_{10}(K)]$ for $\theta = -0.1\pi$ (the left one) and $\theta = 0.1\pi$ (the right one). $w = 10$ is fixed. The OD regions are enclosed by the two critical curves $\tau_1(K, \theta)$ and $\tau_2(K, \theta)$. The open circles represent the numerical results, which well confirm the theoretical prediction.

of the OD regions can be understood intuitively from the different coupling mechanisms induced by the coupling phase. Specifically, for the zero coupling phase $\theta = 0$, the coupling is attractive, which is assumed to prefer an in-phase state; on the contrary, for the coupling phase of $\theta = \pi$ (or $\theta \rightarrow -\pi$), the coupling is repulsive [38], which generally tends to produce an antiphase state. Thus, it is natural to observe that the OD islands vary the way as shown in Fig. 2.

To quantify the above size variation, let $S(\theta)$ denote the area of an OD island on the plane $[\tau, \log_{10}(K)]$ for the coupling phase θ . Obviously, $S(\theta) = 0$ implies that a delay-induced OD is impossible, and $S(\theta) > 0$ means that OD can be induced by suitable parameter sets of (τ, K) . The larger $S(\theta)$, the larger the OD region. Generally, there is no simple way to analytically derive $S(\theta)$, which, however, can easily be

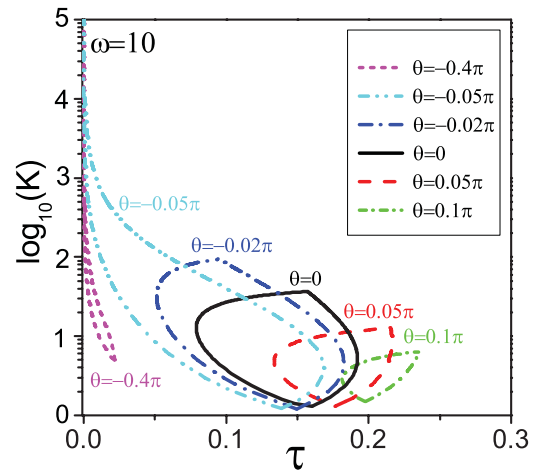


FIG. 2. (Color online) The OD islands of the coupled system (1) in the parameter space $[\tau, \log_{10}(K)]$ for $\theta = -0.4\pi, -0.05\pi, -0.02\pi, 0, 0.05\pi$, and 0.1π , respectively, $w = 10$. All the OD islands, which have been proved by the direct numerical experiments, come from Eq. (3). The OD boundaries are indicated by the different colors and styles of lines.

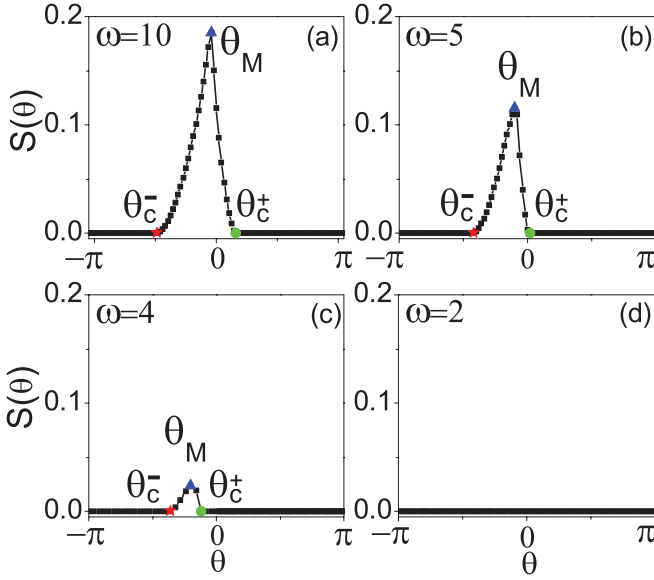


FIG. 3. (Color online) (a)–(d) The OD island area $S(\theta)$ of coupled system (1) vs the coupling phase θ for $\omega = 10, 5, 4$, and 2 , respectively. The maximum point $S(\theta_M)$ at the optimal phase θ_M is indicated by blue triangles, and the two critical points with θ_c^- and θ_c^+ are indicated by red stars and green circles. OD only is possible for $\theta_c^- < \theta < \theta_c^+$.

obtained numerically. The numerical results are depicted in Figs. 3(a)–3(d) with $w = 10, 5, 4$, and 2 , respectively. In Figs. 3(a)–3(c), $S(\theta)$ can always gain its maximum value $S(\theta_M)$ [$S(\theta_M) > 0$] at an optimal coupling phase θ_M ($\theta_M < 0$) and monotonically decreases from $S(\theta_M)$ to zero by altering θ from θ_M to θ_c^+ (or to θ_c^-). A delay-induced OD only is possible for $\theta_c^- < \theta < \theta_c^+$. We find the lower the frequency w , the narrower this interval. For a sufficiently low frequency w , the interval will vanish completely, i.e., $S(\theta) = 0$ for $-\pi < \theta \leq \pi$ [Fig. 3(d) for $w = 2$]. This observation implies that OD can be induced by a delay only if w is beyond a critical value w_c ($w_c > 2$), whose value is given below. These critical behaviors indicate that the delay-induced OD can be controlled by the coupling phase. Note that θ_c^+ , θ_c^- , and θ_M are different for different w 's (Fig. 3).

In Fig. 4(a), we further plot the numerical calculations of θ_c^- and θ_c^+ vs w , which are indicated by solid squares and open squares, respectively. It can be seen that θ_c^+ and θ_c^- originate from the same critical point (w_c, θ_c) . With a further increase in w from w_c , the value of θ_c^+ (θ_c^-) monotonically increases (decreases) and asymptotically approaches $\frac{\pi}{2}$ ($-\frac{\pi}{2}$). Then, the largest death interval (θ_c^-, θ_c^+) is assumed to be $(-\frac{\pi}{2}, \frac{\pi}{2})$ as w goes to infinity.

In fact, the largest death interval of $(-\frac{\pi}{2}, \frac{\pi}{2})$ can be confirmed analytically. OD can occur in the coupled system (1) only if all eigenvalues of the associated characteristic equation have negative real parts, which, in turn, implies that the real part of the trace of the stability matrix M [Eq. (2)] should be negative, i.e., $2(1 - K \cos \theta) < 0$. Because the coupling strength always is positive (i.e., $K > 0$), $\cos \theta > \frac{1}{K} > 0$ holds. Thus, the necessary condition for the OD state is $-\frac{\pi}{2} < \theta < \frac{\pi}{2}$, which proves that the largest death interval cannot be beyond $(-\frac{\pi}{2}, \frac{\pi}{2})$.

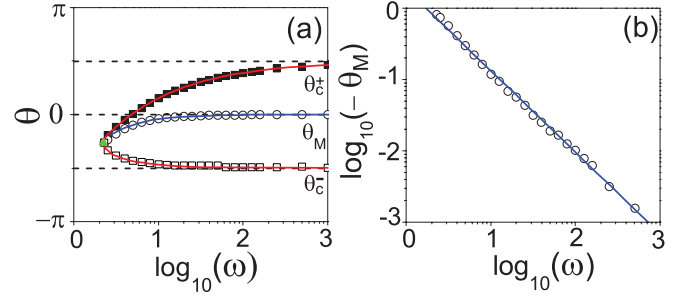


FIG. 4. (Color online) (a) The two critical coupling phases θ_c^- (open squares) and θ_c^+ (solid squares) and the optimal coupling phase θ_M (open circles) vs w from the numerical calculation results of Fig. 3. The red (outward) line comes from Eq. (4), which well predicts θ_c^- and θ_c^+ . The minimum point is highlighted by a green triangle with $(w_c, \theta_c) = (2.27, -0.26\pi)$. The blue (inside) line is the fit by $\theta_M = \alpha w^\beta$ with $\alpha \approx -2.19$ and $\beta \approx -1.16$. The three horizontal dashed lines from top to bottom are $\theta = \frac{\pi}{2}$, 0 , and $-\frac{\pi}{2}$, respectively. (b) The log-log plot of $-\theta_M$ vs w , which shows a perfect power law scaling. The blue line is a linear fit.

Next, we give a prediction of θ_c^- and θ_c^+ . From Fig. 4(a), it can be seen that, for the occurrence of OD, the frequency w should be beyond a certain threshold $w_{\min}(\theta)$. This value can be worked out from the intersection condition of the two critical curves, Eq. (3). By comparing the forms of the two curves, Eq. (3), and supposing that they have, at least, one intersection point, $w_{\min}(\theta)$ is obtained analytically as

$$w_{\min}(\theta) = \min \left\{ \frac{(\pi + 2\theta)\sqrt{K^2 - (K \cos \theta - 1)^2}}{\pi - 2 \cos^{-1} \left(\frac{K \cos \theta - 1}{K} \right)} + \frac{[\pi - 2 \cos^{-1} \left(\frac{K \cos \theta - 1}{K} \right)] K \sin \theta}{\pi - 2 \cos^{-1} \left(\frac{K \cos \theta - 1}{K} \right)}, K > \frac{1}{\cos \theta} \right\}, \quad (4)$$

where $-\frac{\pi}{2} < \theta < \frac{\pi}{2}$. This result is plotted by the red (outward) line in Fig. 4(a), which shows a fairly good coincidence with the previous numerical calculations of θ_c^- and θ_c^+ . The highlighted green triangle is the minimum of the red line with the value of $(w_c, \theta_c) = (2.27, -0.26\pi)$. $w_c = \min[w_{\min}(\theta), -\frac{\pi}{2} < \theta < \frac{\pi}{2}]$. The smallest threshold $w_c = w_{\min}(\theta_c) = 2.27$ is much lower than in the case of the zero coupling phase with the threshold $w_{\min}(\theta = 0) = 4.1812$ numerically found in Ref. [15]. The existence of the critical frequency w_c can be explained physically. From a physical point of view, a low frequency w corresponds to a long period of the system. If the frequency is too low, the system has an extremely long period, thus, the delayed effect of coupling could be too weak to induce an OD state.

The numerical calculations of the optimal coupling phase θ_M also are presented in Fig. 4(a) by the open circles. We see that θ_M monotonically increases as w increases and approaches zero for infinitely large w . Here, it is impossible to analytically deduce the explicit function of θ_M on w . Interestingly, by the numerical fit between $-\theta_M$ and w in the log-log plot [see Fig. 4(b)], we find the following power law relation:

$$\theta_M = \alpha w^\beta, \quad (5)$$

with $\alpha \approx -2.19$ and $\beta \approx -1.16$, which is plotted by the blue (inside) line in Fig. 4(a).

III. NETWORKED DELAY-COUPLED OSCILLATORS

More interestingly, the controlling effects of the coupling phase on the delay-induced OD can be extended to a network of delay-coupled oscillators. Let us consider a network of N delay-coupled Landau-Stuart oscillators,

$$\dot{z}_j(t) = [1 + iw - |z_j(t)|^2]z_j(t) + \frac{K e^{i\theta}}{d_j} \times \sum_{\substack{s=1 \\ s \neq j}}^N g_{js} [z_s(t - \tau) - z_j(t)], \quad (6)$$

where $j = 1, \dots, N$. The coupling topology is governed by g_{js} as follows: If oscillators j and s are connected by a link, then $g_{js} = g_{sj} = 1$; otherwise $g_{js} = g_{sj} = 0$. Self-connections are not allowed, that is, $g_{jj} = 0$. And $d_j = \sum_{s=1}^N g_{js}$ is the degree of node j . Let λ_j 's be the eigenvalues of the networked matrix $G = (\frac{g_{js}}{d_j})_{N \times N}$, ordered as $1.0 = \lambda_1 \geq \lambda_2 \geq \dots \geq \lambda_N \geq -1.0$ [28]. A linear stability analysis of Eq. (6) can be carried out around the OD state $z_1 = z_2 = \dots = z_N = 0$. After some algebraic manipulations, the stability of the OD state is determined by the following N characteristic equations:

$$\lambda = 1 + iw - K e^{i\theta} + K e^{i\theta} \lambda_j e^{-\lambda \tau}, \quad (7)$$

where $j = 1, 2, \dots, N$. By exploring the qualitative dependence of $\text{Re}(\lambda)$ on λ_j , it can be analyzed that the final OD regions only are determined by the two extreme values of λ_1 ($\lambda_1 = 1$) and λ_N . The OD regions finally are determined by the following four critical curves:

$$\begin{aligned} \tau_a(K, \theta) &= \frac{\theta + \cos^{-1} \left(\frac{K \cos \theta - 1}{K} \right)}{w - K \sin \theta - \sqrt{K^2 - (K \cos \theta - 1)^2}}, \\ \tau_b(K, \theta) &= \frac{2\pi + \theta - \cos^{-1} \left(\frac{K \cos \theta - 1}{K} \right)}{w - K \sin \theta + \sqrt{K^2 - (K \cos \theta - 1)^2}}, \\ \tau_c(K, \theta) &= \frac{2\pi + \theta - \cos^{-1} \left(\frac{K \cos \theta - 1}{K \lambda_N} \right)}{w - K \sin \theta - \sqrt{(K \lambda_N)^2 - (K \cos \theta - 1)^2}}, \\ \tau_d(K, \theta) &= \frac{\theta + \cos^{-1} \left(\frac{K \cos \theta - 1}{K \lambda_N} \right)}{w - K \sin \theta + \sqrt{(K \lambda_N)^2 - (K \cos \theta - 1)^2}}. \end{aligned} \quad (8)$$

Clearly, for a given network, its smallest eigenvalue λ_N of the corresponding matrix G completely characterizes the OD regions. The validity of Eq. (8) has been tested by many numerical experiments with networks of different topologies, which coincide with our theoretical analyses very well. In the numerical simulations of networked delay-coupled oscillators, the coupling phase θ is found to play a similar role as in the two delay-coupled oscillators of Eq. (1). In what follows, we exemplarily study one type of regular network and one type of irregular network, respectively.

For a regular network, here, we consider a typical ring network with a nearest-neighbor connection, for which the

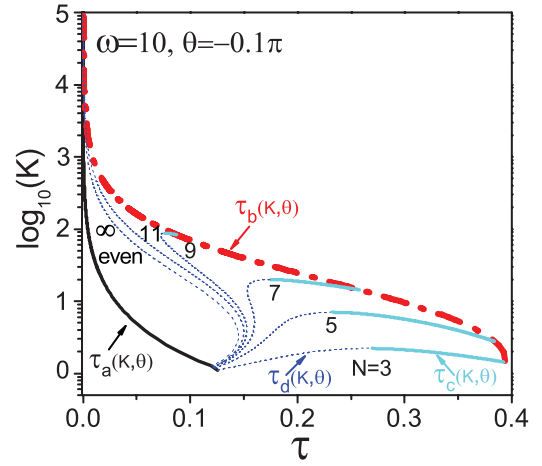


FIG. 5. (Color online) The OD islands of the coupled system Eq. (6) with a ring network for different coupled oscillators N . The OD islands remain unchanged for all the ring networks with even nodes N . For the odd values N , the OD regions are enclosed by four critical curves when $N \leq 9$, and two curves otherwise, and as $N \rightarrow \infty$, the OD boundaries approach that for the even N . $\theta = -0.1\pi$ and $\omega = 10$ are fixed. The four critical curves are indicated by the different colors and styles of lines.

smallest eigenvalue λ_N of the network matrix can be obtained analytically as follows:

$$\lambda_N = \begin{cases} -1.0, & \text{if } N \text{ is even,} \\ \cos \left[\left(1 - \frac{1}{N} \right) \pi \right], & \text{if } N \text{ is odd.} \end{cases} \quad (9)$$

Then, by calculating the four critical curves in Eq. (8) with $\theta = -0.1\pi$ and different N 's, the OD islands are shown in Fig. 5. All ring networks with even N nodes have the same OD island. In the case of odd N , the OD islands decrease as N increases and approach that of even N as N approaches infinity. This behavior is similar as in the case of the zero coupling

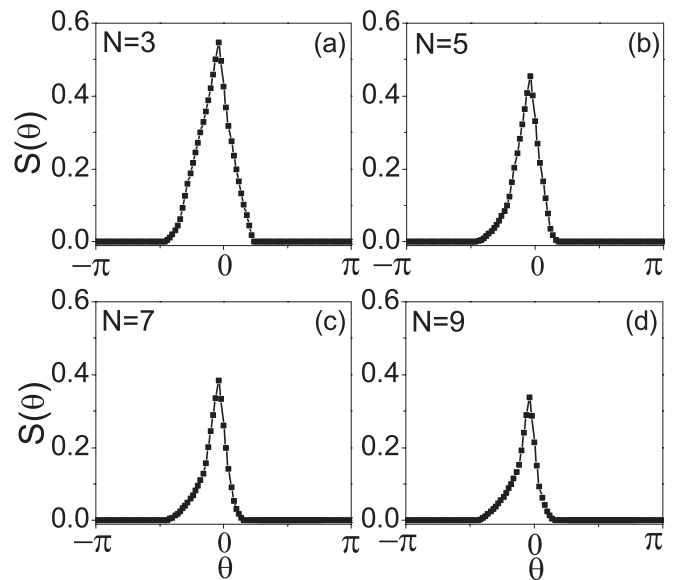


FIG. 6. (a)–(d) The OD island area $S(\theta)$ vs the coupling phase θ for a ring of delay-coupled Landau-Stuart oscillators with $N = 3, 5, 7$, and 9 , respectively, $\omega = 10$. The structure is quite similar to that in Fig. 3.

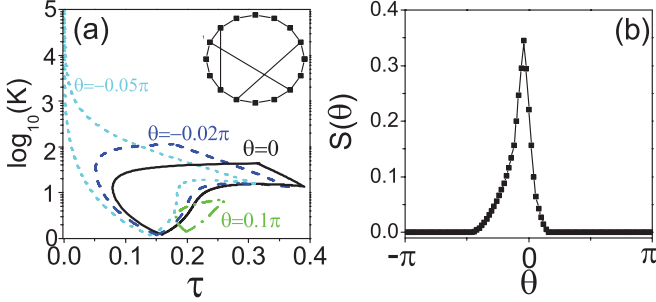


FIG. 7. (Color online) (a) The OD islands of the coupled system Eq. (6) with the irregular network for different coupling phases θ . The OD boundaries are indicated by the different colors and styles of lines. A schematic of the irregular network structure is depicted in the upper-right corner. (b) The OD island area $S(\theta)$ vs θ for the irregular network used in (a). Also, the structure is quite similar to that in Fig. 3. $\omega = 10$ is fixed.

phase $\theta = 0$ observed in coupled limit-cycle oscillators [16] and in coupled chaotic Rössler oscillators [29]. To reveal the effect of the coupling phase on the OD regions, the simulation results of $S(\theta)$ vs θ are provided in Figs. 6(a)–6(d) for $N = 3, 5, 7$, and 9 , respectively. These patterns strongly resemble the structures in Fig. 3, which affirm the importance of the coupling phase for control in the regular network.

For a general irregular network, although its smallest eigenvalue λ_N of the corresponding matrix G cannot be derived analytically, it can be computed numerically. Once λ_N is known for an irregular network, its OD regions easily can be obtained from Eq. (8). As an illustrated example, here, we construct a small-size irregular network by randomly adding three edges on an initial ring network with $N = 16$ nodes. A scheme of the network topology is illustrated in the upper-right corner of Fig. 7(a). The λ_N for this irregular network is -0.9430 . Several OD islands of the irregular network for different coupling phases are depicted in Fig. 7(a), which are obtained by calculating the curves of Eq. (8) and are checked by direct numerical integration. From the results shown in Fig. 7(b), again, we find that, by tuning the coupling phase θ , the OD islands change in a similar way as previously observed in the two delay-coupled oscillators, Eq. (1). The pattern in Fig. 7(b) clearly shows the crucial role of the coupling phase in controlling OD dynamics in the irregular network.

IV. CONCLUSION AND DISCUSSIONS

In conclusion, we have shown that the coupling phase parameter enables us to control the stability domains of delay-induced OD in coupled oscillators. For a frequency w beyond the critical value w_c , the delay-induced OD only is possible for a coupling phase θ located in the interval of (θ_c^-, θ_c^+) , which monotonically increases with the increase in w and approaches $(-\frac{\pi}{2}, \frac{\pi}{2})$ for sufficiently large w . The optimal coupling phase θ_M , for which the OD island is maximal, is well characterized by a power law scaling relation with the frequency w . The controlling function of the coupling phase is extended to a general delay-coupled network. It is notable that, to carry out a complete analysis, the described results are presented in the context of coupled Landau-Stuart

limit-cycle oscillators. Also, the generality is confirmed well by numerical experiments of delay-coupled chaotic oscillators with the coupling phase [35]. We expect that all findings in this paper are of significance for the control of oscillating dynamics and can provide a positive inducement for various experimental studies in the future.

Finally, it is valuable to give some further discussions.

(1) The main difference between the delayed feedback control and our method is as follows. The phenomenon OD refers to stabilizing an unstable steady state by the coupling between, at least, two autonomous oscillators. The self-sustained oscillations of coupled oscillators are quenched by the interactions between oscillators. This is quite different from controlling an unstable focus in one delayed feedback oscillator [39–41] where the oscillations are suppressed by the feedback information of the system itself. Besides, the OD regions generally depend on the number N ($N \geq 2$) of coupled oscillators, see Eq. (8) and the results shown in Fig. 5.

(2) Our analyses have shown that the OD island is determined by three factors: the frequency w , the coupling phase θ , and the smallest eigenvalue λ_N of the networked matrix. One may obtain the same results by starting from the delay-coupled unstable focus without any limit cycle [4]. But, it would be physically more significant to consider a complete model with oscillating (periodic or chaotic) behavior, which contains all the necessary structures to reveal the novel effects induced by delayed coupling in real systems.

(3) The boundaries of the OD regions are derived by performing a standard linear stability analysis of the coupled systems around the unstable origin, whose global stability is extremely difficult to study. In practice, to numerically check the OD regions, random initial conditions have been adopted in all the experiments. The employed numerical technique signals that the OD state is not only locally, but also globally stable. The limit cycle is completely lost in the OD regions for all the randomly chosen initial conditions, which is supposed to be observed generally for the system near a Hopf bifurcation.

(4) It has been identified that, besides the coupling phase θ , the system parameter w also acts as a crucial quantity. This parameter characterizes the period $T = \frac{2\pi}{w}$ of the uncoupled limit cycle, which also sets the intrinsic time scale of the unstable fixed point. Hence, considering their relationship with the time delay, the results may stand without explicit knowledge of the system's parameters. This constitutes our future papers.

ACKNOWLEDGMENTS

W.Z. was supported by the National Natural Science Foundation of China (NSFC) under Grant No. 11147179, the Fundamental Research Funds for the Central Universities of China under Grant No. 2011QN161, and the Alexander von Humboldt Foundation. J.L. was supported by the National Natural Science Foundation of China (NSFC) under Grants No. 11026182 and No. 61175119, the Natural Science Foundation of Jiangsu Province of China under Grant No. BK2010408, the Program for New Century Excellent Talents in University (Grant No. NCET-10-0329), and the Alexander von Humboldt Foundation. Y.T. was supported by the National Natural Science Foundation of China (NSFC) under Grant No.

60874113 and the Alexander von Humboldt Foundation. C.Z. was supported by the National Natural Science Foundation of China (NSFC) under Grant No. 11171125. J.K. was supported

by SUMO (EU) and ECONS (WGL). We appreciate the anonymous reviewers for their very thoughtful comments that helped to greatly improve this paper.

-
- [1] A. T. Winfree, *The Geometry of Biological Time* (Springer-Verlag, New York, 1980).
 - [2] Y. Kuramoto, *Chemical Oscillations, Waves, and Turbulence* (Springer, Berlin, 1984).
 - [3] *Handbook of Chaos Control*, edited by E. Schöll and H. G. Schuster, second completely revised and enlarged edition (Wiley-VCH, Weinheim, 2008)
 - [4] P. Hövel, *Springer Theses Recognizing Outstanding Ph.D. Research* (Springer-Verlag, Berlin Heidelberg, 2010).
 - [5] A. Arenas, A. Díaz-Guilera, J. Kurths, Y. Moreno, and C. Zhou, *Phys. Rep.* **469**, 93 (2008).
 - [6] E. Ullner, A. Zaikin, E. I. Volkov, and J. García-Ojalvo, *Phys. Rev. Lett.* **99**, 148103 (2007).
 - [7] A. Koseska, E. Volkov, and J. Kurths, *Europhys. Lett.* **85**, 28002 (2009).
 - [8] A. F. Taylor, M. R. Tinsley, F. Wang, Z. Y. Huang, and K. Showalter, *Science* **323**, 614 (2009).
 - [9] R. E. Mirollo and S. H. Strogatz, *J. Stat. Phys.* **60**, 245 (1989).
 - [10] D. G. Aronson, G. B. Ermentrout, and N. Kopell, *Physica D* **41**, 403 (1990).
 - [11] L. Rubchinsky and M. Sushchik, *Phys. Rev. E* **62**, 6440 (2000).
 - [12] J. Yang, *Phys. Rev. E* **76**, 016204 (2007).
 - [13] W. Liu, X. Wang, S. Guan, and C.-H. Lai, *New J. Phys.* **11**, 093016 (2009).
 - [14] D. V. Ramana Reddy, A. Sen, and G. L. Johnston, *Phys. Rev. Lett.* **80**, 5109 (1998).
 - [15] D. V. Ramana Reddy, A. Sen, and G. L. Johnston, *Physica D* **129**, 15 (1999).
 - [16] R. Dodla, A. Sen, and G. L. Johnston, *Phys. Rev. E* **69**, 056217 (2004).
 - [17] K. Konishi, *Phys. Rev. E* **68**, 067202 (2003).
 - [18] R. Karnatak, R. Ramaswamy, and A. Prasad, *Phys. Rev. E* **76**, 035201(R) (2007).
 - [19] W. Zou, X. G. Wang, Q. Zhao, and M. Zhan, *Fron. Phys. China* **4**, 97 (2009).
 - [20] D. V. Ramana Reddy, A. Sen, and G. L. Johnston, *Phys. Rev. Lett.* **85**, 3381 (2000).
 - [21] A. Takamatsu, T. Fujii, and I. Endo, *Phys. Rev. Lett.* **85**, 2026 (2000).
 - [22] R. Herrero, M. Figueras, J. Rius, F. Pi, and G. Orriols, *Phys. Rev. Lett.* **84**, 5312 (2000).
 - [23] A. Prasad, Y. C. Lai, A. Gavrielides, and V. Kovanis, *Phys. Lett. A* **318**, 71 (2003).
 - [24] F. M. Atay, *Phys. Rev. Lett.* **91**, 094101 (2003).
 - [25] W. Zou and M. Zhan, *Phys. Rev. E* **80**, 065204(R) (2009).
 - [26] W. Zou, C. G. Yao, and M. Zhan, *Phys. Rev. E* **82**, 056203 (2010).
 - [27] G. Saxena, A. Prasad, and R. Ramaswamy, *Phys. Rev. E* **82**, 017201 (2010).
 - [28] F. M. Atay, *Physica D* **183**, 1 (2003).
 - [29] W. Zou, X. Zheng, and M. Zhan, *Chaos* **21**, 023130 (2011).
 - [30] B. Fiedler, V. Flunkert, P. Hövel, and E. Schöll, *Philos. Trans. R. Soc. London, Ser. A* **368**, 319 (2010).
 - [31] S. Schikora, P. Hövel, H.-J. Wünsche, E. Schöll, and F. Henneberger, *Phys. Rev. Lett.* **97**, 213902 (2006).
 - [32] Z. Jiang and M. McCall, *J. Opt. Soc. Am. B* **10**, 155 (1993).
 - [33] M. Rosenblum and A. Pikovsky, *Phys. Rev. E* **70**, 041904 (2004).
 - [34] B. Fiedler, V. Flunkert, M. Georgi, P. Hövel, and E. Schöll, *Phys. Rev. Lett.* **98**, 114101 (2007).
 - [35] K. Pyragas and T. Pyragiene, *Phys. Rev. E* **78**, 046217 (2008).
 - [36] C.-U. Choe, T. Dahms, P. Hövel, and E. Schöll, *Phys. Rev. E* **81**, 025205(R) (2010).
 - [37] C.-U. Choe, V. Flunkert, P. Hövel, H. Benner, and E. Schöll, *Phys. Rev. E* **75**, 046206 (2007).
 - [38] L. S. Tsimring, N. F. Rulkov, M. L. Larsen, and M. Gabbay, *Phys. Rev. Lett.* **95**, 014101 (2005).
 - [39] A. G. Balanov, N. B. Janson, and E. Schöll, *Phys. Rev. E* **71**, 016222 (2005).
 - [40] S. Yanchuk, M. Wolfrum, P. Hövel, and E. Schöll, *Phys. Rev. E* **74**, 026201 (2006).
 - [41] T. Dahms, P. Hövel, and E. Schöll, *Phys. Rev. E* **76**, 056201 (2007).